Chapter 1
Introduction

Sebastian Volz

1.1 Nanostructures

Nanomaterials are defined here to be composites of entities with characteristic sizes in the range 0.1–500 nm, dilute or dense, capable of significantly modifying the properties of the matrix. These elements, called nanostructures, make up a five-letter 'alphabet': nanofilms, superlattices (Fig. 1.1a, stacks of nanofilms), nanowires (Fig. 1.1b), nanotubes (Fig. 1.1c), and nanoparticles (Fig. 1.1d).

These structures are synthesised either by relatively accessible chemical processes, e.g., electrochemistry, emulsions, milling, etc., or else by techniques involving large scale and costly equipment, e.g., molecular beam epitaxy (MBE) or focussed ion beams (FIB). Plasma deposition and chemical vapour deposition (CVD) chambers have a somewhat intermediate status, given that masking and etching may involve heavy investment when a high resolution is required.

Nanostructures have very different properties to macroscopic materials. These properties are usually related to mechanisms belonging to macroscopic physics. A nanowire can have a thermal conductivity 100 times lower than the bulk material [1], and a nanotube has higher thermal conductivity than diamond [2], if it is definable at all. This kind of extreme behaviour is an incentive to creating new composites whose properties would be modulated by varying the density, nature, and ordering of the included nanostructures.

Naturally, an isolated nano-object has very different properties from one that is included within a matrix. With the change of scale, the absence of percolation and the contact resistance between the structures and the matrix on the one hand and between the structures themselves on the other mean that intrinsic properties are not conserved. In order to control the effective properties of the resulting materials, it is thus essential to understand these resistances and the overall organisation of the constituent nano-objects.

Another approach here is simply to integrate a single nanostructure within a micro- or nanosystem to set up some function with a minimum amount of matter

S. Volz (ed.), *Thermal Nanosystems and Nanomaterials*, Topics in Applied Physics, 118
DOI 10.1007/978-3-642-04258-4_1,

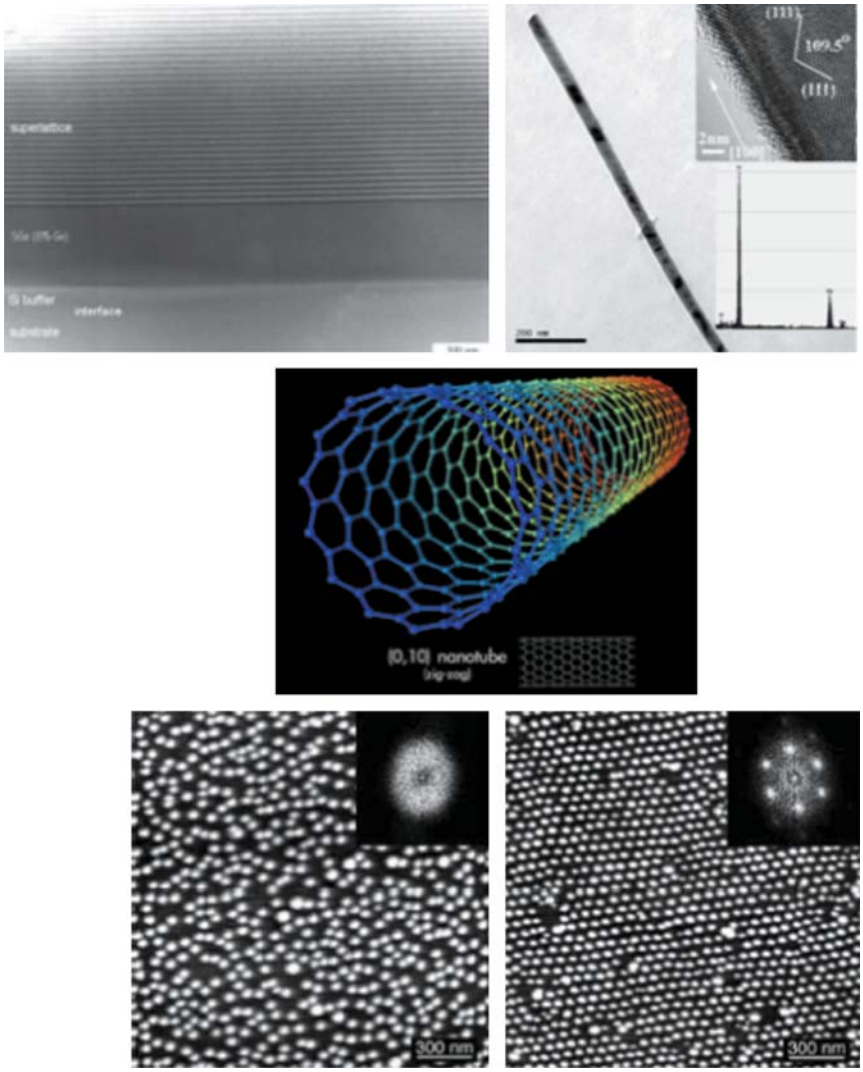

Fig. 1.1 *Top left*: Transmission electron microscope image of an Si/SiGe superlattice (Paul Schereer Institute). *Top right*: Transmission electron microscope image of a silicon nanowire. *Insert*: Magnification of the surface of the wire. *Center*: Image showing the structure of a single-wall carbon nanotube (University of Liège). *Bottom*: Atomic force microscope images of a monolayer of PbSe nanoparticles. *Inserts* show the 2D spectra of the images which reveal the ordering into hexagonal structures

and on a much reduced surface area. The original aim of nanotechnology was to assemble atoms together to build up molecules that could carry out some precise function in such a way as to save on the amount of material and ensure the sustainable development of contemporary electronics and telecommunications.

This approach was not continued for political reasons, but the pursuit of miniaturisation has nevertheless led to a drastic reduction in the dimensions of technological systems.[1] In 2008, an electronic chip with surface area around 1 cm^2 contains 250 million transistors (45 nm technology) and 6 km of interconnect tracks. In 2020, this same chip should carry as many transistors as the brain contains neurons.

In this first chapter of Part I, we present the various thermal applications of nanomaterials, then discuss the physical mechanisms underlying the novel properties of nanostructures.

1.2 Scientific and Technological Stakes

Thermal applications are currently being developed for the purposes of insulation, comfort, cooling, and also energy conversion. For example, aerogels are ultraporous media made up of fibres, themselves resulting from the coalescence of silica nanoparticles. By packing these materials in vacuum, their thermal conductivity can be made smaller than the thermal conductivity of air [3]. Figure 1.2a shows the equivalent thickness of rock wool needed to achieve the same result as an aerogel panel.

Phase-change microcapsules represent a huge market in the context of technical textiles (see Fig. 1.3). Phase-change materials provide a way of imposing a constant

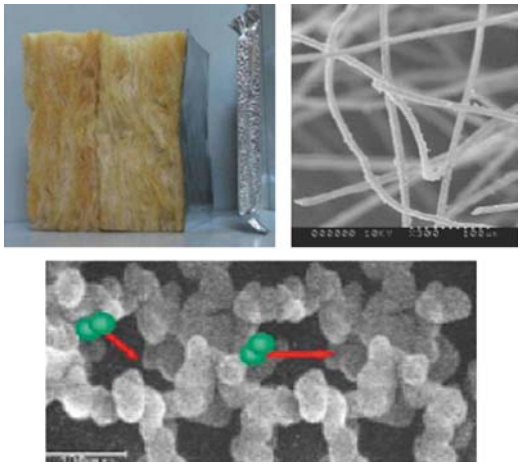

Fig. 1.2 *Top left*: Thickness of rock wool need to achieve the thermal insulation produced by an aerogel panel. *Top right*: Aerogel fibre with porosity greater than 90%. *Bottom*: Silica nanoparticle structure (CSTB)

[1] Apart from savings of raw materials, miniaturisation can increase operating speeds because electrons travel shorter distances, and it can reduce the heat power dissipated for a given amount of data because interconnect resistances and operating currents in transistors decrease with size.

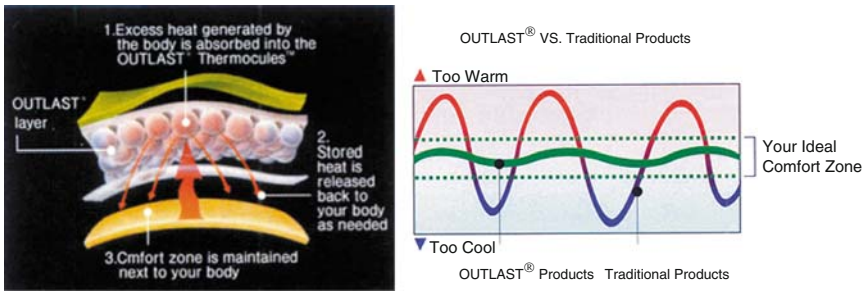

Fig. 1.3 *Left*: Structure of a cloth equipped with phase-change microcapsules called Thermocules. *Right*: Qualitative representation of temperature levels with (*green curve*) and without (*red and blue curve*) microcapsules

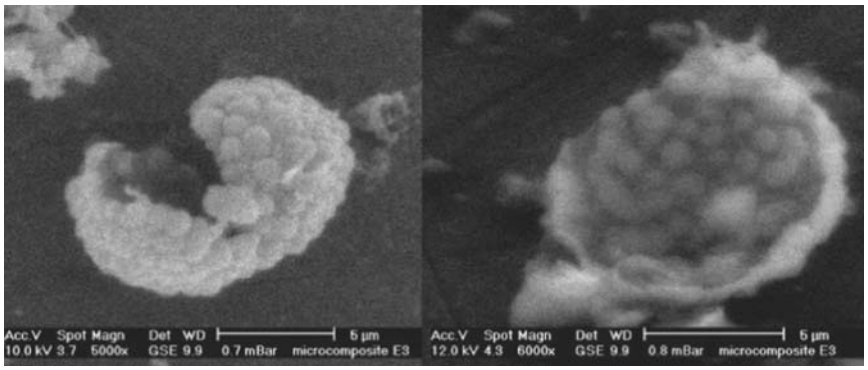

Fig. 1.4 Scanning electron microscope images of a packet of phase-change microcapsules. LGMT Roubaix

temperature, or with only slight variations, in response to changes in internal or external conditions. The phase change requires encapsulation (see Fig. 1.4), and the micron or submicron size of the capsules is what allows fast phase changes to occur.

A major aim for the semiconductor industry is the cooling of chips in microelectronics. Strategies are multiscale and varied. There are techniques operating on the scale of the chip itself. A good example is the system of fins of millimeter lengths made up of packets of nanotubes, as shown in Fig. 1.5 [4]. The very high thermal conductivity of the nanotubes makes the fins highly efficient. An increase of 19% has been demonstrated in the extracted power.

Undoubtedly the most exciting field of applications of nanostructures, and the one which has generated the most research and led to the most significant developments, is the area of thermoelectric conversion. Efficient materials for this must have high electrical conductivity and low thermal conductivity. Such paradoxical behaviour can be obtained by reducing the thermal conductivity by introducing nanostructures, e.g., nanoparticles (see Fig. 1.6) [5], nanowires (see Figs. 1.7 and 1.8) [6], or superlattices [7]. The merit factor was increased to 2.4 at room

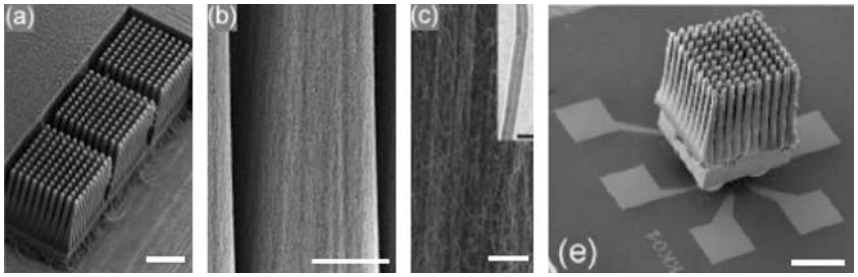

Fig. 1.5 Fins made from nanotubes for cooling electronic components [4]

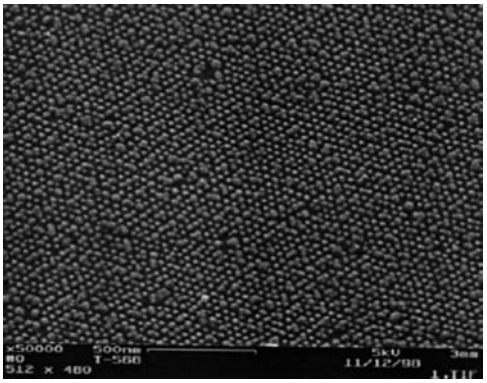

Fig. 1.6 PbSeTe quantum dots deposited by MBE. A merit factor of 1.6 has been achieved at room temperature [5]

temperature, for example, using superlattices, while it had remained below unity during the second half of the twentieth century.

The emerging area of thermal diode nanostructures was largely triggered by recent work by A. Majumdar and coworkers at UC Berkeley [8]. Increasing the mass of one end of a carbon nanotube (see Fig. 1.9) caused an asymmetry in the measured heat fluxes, as shown in Fig. 1.10, where the blue and red curves indicate the flux in the two directions in the tube. This asymmetry, although slight, has many physical implications, since classical thermodynamics and heat transfer forbid such behaviour. One can appeal to wave effects, but the waves commonly considered as heat carriers, viz., phonons, have completely symmetric behaviour when passing through an interface or a body. The paper [8] thus suggests the existence of rather special waves called solitons, likely to occur in a low-dimensional crystal lattice with a non-symmetric transmission factor, i.e., in which the transmitted amplitude depends on the direction of the wave through the crystal.

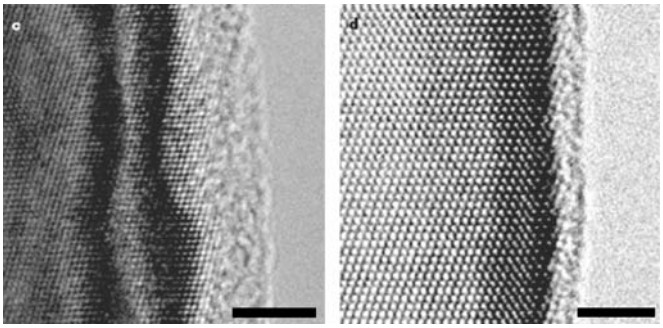

Fig. 1.7 Structural characterisation by scanning electron microscope of rough nanowires. *Left*: High-resolution transmission electron microscope image of a rough wire. The roughness appears between the wire and the native amorphous silica. *Right*: Transmission electron microscope image of an untreated nanowire. *Scale bars* represent 4 nm and 3 nm, respectively

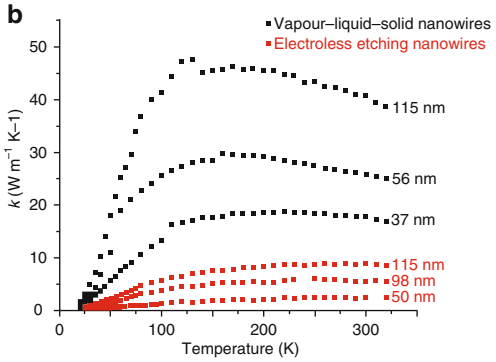

Fig. 1.8 Thermal conductivity of silicon nanowires with smooth surfaces (*black curves*) and chemically etched surfaces (*red curves*). A drop by a factor of 4 to 5 is observed when the surfaces are etched

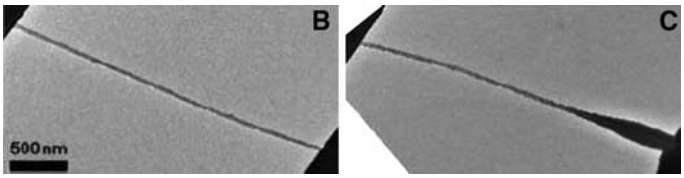

Fig. 1.9 Transmission electron microscope images of a suspended nanotube before (**b**) and after (**c**) adding C9H16Pt [8]

1.3 Physical Mechanisms

Heat conduction in nanostructures is not the same as in macroscopic systems, where it is characterised by Fourier's law. In the latter case, the heat carriers can be visualised as behaving like little beads with Brownian-like trajectories, i.e., suffering

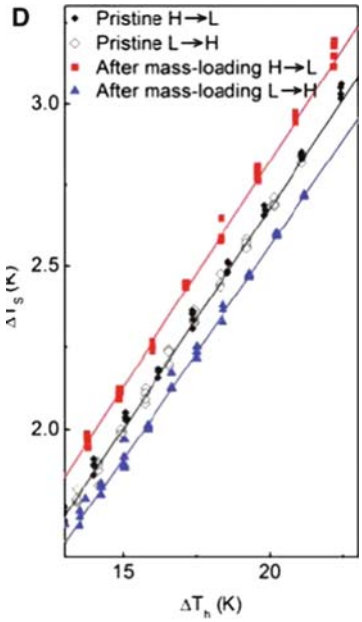

Fig. 1.10 Heat flux passing through a carbon nanotube for different imposed temperatures. When no mass is added to one end of the nanotube, measurements show that there is no difference between the two flow directions (*diamonds*). In contrast, the *blue* and *red curves* reveal this asymmetry when a mass is added to one end of the nanotube

frequent and random changes of direction. These movements are due to collisions between the carriers owing to their high density.

1.3.1 Rarefaction. Surface Reflection and Transmission at Interfaces

However, when this density decreases, the distance travelled by a heat particle between two collisions can exceed the characteristic length scale of the structure. The particle will then enter into more collisions with the walls of the system than with its counterparts within the system. This regime is no longer Brownian, but ballistic, because the particle will basically move in a straight line at constant speed between consecutive reflections from the system walls (see Fig. 1.11).

This is the first non-Fourier effect which could be qualified as a rarefaction phenomenon. The key mechanism here is the reflection of particles at the surface, but also transmission at the interface in the case of joined structures. If the reflection is perfectly specular, for example, the incident energy is fully redistributed in the symmetrical direction, and the flux component parallel to the wall remains unchanged, so there is no effect due to rarefaction in this same direction, even if the characteristic length scale is nanometric. But if now the reflection is diffuse and isotropic, i.e., all the energy is redistributed equally in all directions, a back flux arises and physical properties are modified.

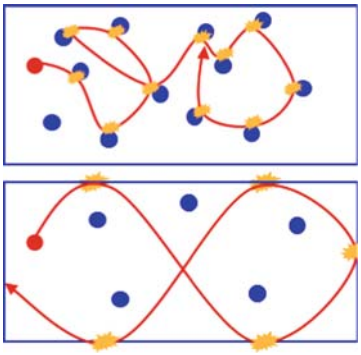

Fig. 1.11 Path of a heat carrying particle (*red blob*) in the diffusive regime (*top*), where the carrier density is high, and in the ballistic regime (*bottom*), where the carrier density is low. The prevailing mechanism in the diffusive case is interparticle interaction. In the ballistic case, it is particle–surface interactions that dominate

In a first approximation, reflection and transmission are assumed to be a linear combination of the two extremes, specular and diffuse. The fraction of the incident energy that is reflected specularly defines a coefficient called the specularity. But while the particle on its straight line path is indeed treated as a particle, it is its wavelike behaviour that governs its reflection or transmission. The specularity coefficient will thus depend on the wavelength and polarisation of the particle, the roughness of the surface, and the angle of incidence. It is therefore impossible to account exhaustively for the full complexity of the physical mechanisms that contribute to this coefficient, and it is generally treated as a floating parameter when computations are carried out.

This first rarefaction effect is often computed using the Boltzmann equation, which expresses the conservation of the number of heat carrying particles. Numerical solution can be based upon a classical approach or a direct method such as Monte Carlo simulation. The weak point in such simulations is the lack of data concerning the mean free path of the calculated mode, but also concerning the specularity coefficient. These methods will be examined in the next chapter.

1.3.2 Confinement

The word ‘particle’ is used to cover the more detailed reality of a localised wave packet. This wave packet is made up of several waves in different resonant or normal modes. It is the mode, the manner of vibration, that contains the energy of the system. It is assumed to be a travelling wave, since the system is a bulk system and much bigger than the lattice constant, i.e., the interatomic distance. The amplitudes u_n of these waves can be modelled by plane monochromatic waves, that is, complex exponentials whose arguments contain the wave vectors k and a time dependence

associated with the frequency ω:

$$u_n = u\mathrm{e}^{\mathrm{i}(kx-\omega t)} \ .$$

When modelling such modes, the boundary conditions are called Born–Von Karman conditions: the wave arriving at one end will come back in by the other. It thus propagates indefinitely in the same direction as long as it does not interact, and it moves at a speed imposed by the speed of the given mode.

Imagine now that the wave amplitude is annihilated at one end. This is what happens, for example, at the bridge of a guitar or when an acoustic wave in a crystal arrives at a free surface. The wave incident at this stopping point will be reflected with reversal of its phase, as shown in Fig. 1.12. The incident and reflected waves can still be modelled by monochromatic plane waves, that is, complex exponentials whose arguments contain wave vectors k with opposite signs, since the waves propagate in opposite directions. Their superposition is thus modelled as a sum of two exponentials, equal to the product of a cosine function whose argument depends on the wave vector and a complex exponential defining the temporal phase:

$$u_n \sim \exp\mathrm{i}(kx-\omega t) + \exp\mathrm{i}(-kx-\omega t) = \cos(kx)\mathrm{e}^{-\mathrm{i}\omega t} \ .$$

The zeros of the cosine function do not depend on time and define the nodes of a stationary wave. The vanishing of the amplitude at the boundary $x = L$ requires $kL = \pi/2 + n2\pi$, where n is an integer.[2] The wavelengths are thus $L/(n+1/4)$, defining the normal modes of the cavity formed by the structure. If the width L varies, then the wavelengths will also vary. New eigenmodes specific to the nanostructure thus form.

This transformation of the travelling normal modes into stationary normal modes is the second non-Fourier effect, referred to as confinement. By definition, these stationary waves have zero propagation speed. As the heat flux is proportional to the speed, the contribution of such stationary modes to heat transfer also vanishes.

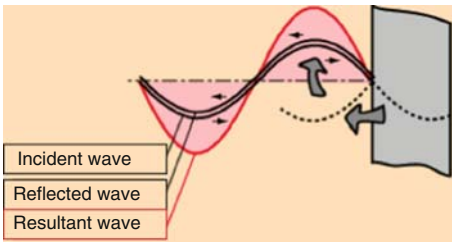

Fig. 1.12 An incident wave (*black line*) reflects (*black line*) on the surface with phase reversal. The superposition of the incident and reflected waves produces a stationary wave of twice the amplitude (*red line*)

[2] The root $n\pi$ not considered here would correspond to an incident wave moving away from the surface.

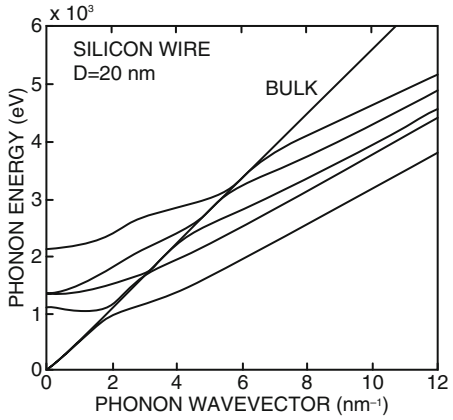

Fig. 1.13 Dispersion curves for the phonons in a silicon nanowire of diameter 20 nm (*continuous lines*). Small slopes and low group velocities correspond to small phonon wave vectors or long wavelengths as a result of confinement. Each branch is related to the projection of an oblique mode onto the wire axis. The bulk dispersion curve is shown by the *dashed line*

The dispersion curves giving the frequency as a function of the wave vector are therefore flat, because their slope is given by the mode speed, as shown in Fig. 1.13.

The second non-Fourier effect is thus determined by calculating these new eigenmodes. Analytical or numerical solutions of the elasticity equation can be implemented. They assume that the atomic motions can be treated as deformations of the crystal, itself treated as a continuum. This hypothesis remains doubtful for modes with short wavelengths. Approaches describing the motion of the atoms, such as lattice dynamics and molecular dynamics, remain more reliable but more difficult to apply at scales exceeding about ten nanometers.

1.3.3 Densities of States and Dimensionality

As can be seen from Fig. 1.13, confinement modifies the distribution of the modes as a function of frequency. The number of modes in a given frequency interval $[w, w+\mathrm{d}w]$ or wave vector interval $[\mathbf{k}, \mathbf{k}+\mathrm{d}^3\mathbf{k}]$ is called the density of states $D(\omega)$ or $D(k)$, respectively.

The directions of the vibrations in a crystal cover the whole space, and so do the directions of the wave vectors. The density of states in the bulk is thus proportional to a volume element, let us say an element in the form of a spherical shell, i.e., $D(k) \propto k^2 \mathrm{d}k$. If now the vibrations only build up in two dimensions, as in a graphene film, the density of states is proportional to a surface element, i.e., $D(k) \propto k\mathrm{d}k$. Finally, in the case of a nanowire, where the vibrations can only propagate in one direction, the density of states is proportional to a length element, i.e., $D(k) \propto \mathrm{d}k$.

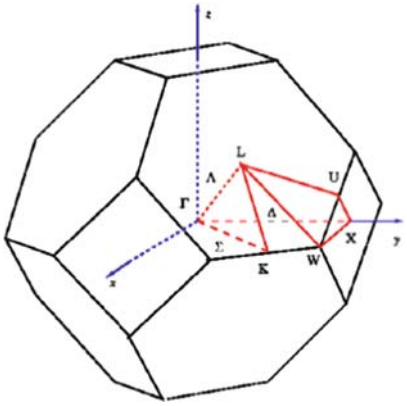

Fig. 1.14 Brillouin zone of an fcc crystal: the volume specified by the set of wave vectors of a bulk crystal. The space beyond this volume corresponds to wavelengths that are too short to be represented by the atoms of the crystal

In short, it can be shown that $D(k) = k^{d-1}\mathrm{d}k$, where d is the dimension of the structure. Since the thermal conductivity is proportional to the heat capacity, and hence to the density of states, the dimensionality of the structure has a significant impact on heat transfer. This is the third non-Fourier effect.

1.3.4 Non-Fourier Effects and Thermal Conductivity

In order to put the three non-Fourier effects into perspective, we shall establish a little known expression for the thermal conductivity [9] which contrasts the effect of the relaxation time, associated with the rarefaction phenomenon, and the effect of the density of states, reflecting confinement and the dimensionality of the structure.

We begin with an expression for the heat flux q:

$$q = \sum_k n_k \hbar \omega_k v_k \,, \tag{1.1}$$

taken as the product of the energy of mode k, i.e., the number n_k of particles in the mode multiplied by the energy $\hbar\omega_k$ of each such particle, and the group velocity v_k of mode k. This expression can be inserted into the Green–Kubo formula for the thermal conductivity [10], viz.,

$$\lambda = \frac{1}{V k_\mathrm{B} T^2} \int_0^\infty \big\langle q(0) q(t) \big\rangle \mathrm{d}t \,, \tag{1.2}$$

where V is the volume and k_B the Boltzmann constant, whence

$$\lambda = \frac{1}{Vk_{\mathrm{B}}T^2}\int_0^\infty \mathrm{d}t \sum_k \left\langle n_k(0)n_k(t)\right\rangle (\hbar\omega_k v_k)^2$$
$$\propto \int_0^\infty \mathrm{d}t \int_k \mathrm{d}k (\hbar\omega_k v_k)^2 \left\langle n_k(0)^2\right\rangle \mathrm{e}^{-t/\tau_k} k^{d-1} \,. \tag{1.3}$$

The relaxation time has been denoted by τ_k. Here, cross-products between different modes have been dropped and the time dependence of the autocorrelation of the particle number has been expressed exactly [11]. The transition from a discrete sum to an integral[3] has brought in the density of states $k^{d-1}\mathrm{d}k$. To simplify, (1.3) is taken in the classical limit $n_k\hbar\omega_k = k_{\mathrm{B}}T$. If the relaxation time $\tau_k = Ck^{-\delta}$, where δ can be viewed as the attenuation of mode k, then using the change of variable $u = tCk^{\delta}$, it follows that

$$\lambda \propto \int_0^\infty \mathrm{d}t \int_k \mathrm{d}k\, \mathrm{e}^{-t/\tau_k} k^{d-1} \propto \frac{1}{1-d/\delta}\left[t^{1-d/\delta}\right]_{t_{\min}}^{\infty} \,. \tag{1.4}$$

A minimal cutoff time $t_{\min}$, corresponding for example to the period of the fastest mode, has been introduced.

The Debye approximation is introduced in such a way that the group velocity can be treated as independent of the wave vector k and taken out as a constant factor. This is a rather crude approximation, because it ignores confinement, which should be taken into account through low group velocities that depend on the wave vector.[4]

If $d > \delta$, (1.4) becomes $t_{\min}^{1-d/\delta}/(1-d/\delta)$. This is shown in Fig. 1.15. The situation for the bulk material ($d = 3$, $d = 2$) and the possible case of a nanotube ($d = 2$, $\delta = 2$) are indicated. Figure 1.15 shows that, moving toward low values of d/δ, i.e., when the dimension of the structure decreases or the attenuation of the mode

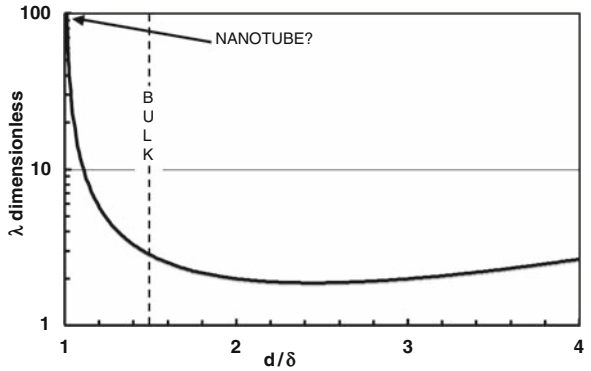

Fig. 1.15 Thermal conductivity as a function of the ratio d/δ, when $d > \delta$

[3] Note that the time integral of (1.3) leads to the well known formula $\lambda = \sum_k C_k v_k^2 \tau_k$ for the thermal conductivity, analogous to the result from kinetic theory.

[4] The increase in the number of branches due to confinement could be fairly easily accounted for by a sum over the branches of the result obtained, in which the constants C and δ would take different values in the different branches.

increases, the conductivity increases and even diverges. Moving toward high values of d/δ, the conductivity decreases to a minimum, then increases again. The two trends of increase and decrease can be put down to competition between attenuation and the reduction in the number of modes. If on the other hand $d = \delta$ or $d > \delta$, (1.4) clearly shows that the thermal conductivity becomes infinite.

1.4 Conclusion

An understanding of the way heat transfers in nanostructures will open the way to applications in the field of transport physics – typically using the Boltzmann equation and the description of rarefied regimes – and also in the field of solid-state physics – with the equation for atomic motions and phonon densities of states and dispersion curves. The various physical phenomena coming into play can lead to opposing trends for thermal properties. In a nanowire, for example, the thermal conductance is greatly reduced in comparison with its value in the bulk, while it is greatly increased in a single-wall nanotube.

In the next two chapters, the physics of the mechanisms introduced in this chapter is explored in more detail, and methods of solution are applied to establish quantitative properties of the basic nanostructures, viz., films, wires, and tubes.

References

1. S. Volz, G. Chen: Appl. Phys. Lett. **57**, 2056 (1999)
2. N. Mingo, D.A. Broido: Phys. Rev. Lett. **95**, 096105, 2005
3. G. Domingues, D. Rochais, S. Volz: J. Comp. Theor. NanoSc. **5**, 2, 153 (2008)
4. K. Kordás, G. Tóth, P. Moilanen, M. Kumpumäki, J. Vähäkangas, A. Uusimäki, R. Vajtai, P.M. Ajayan: Appl. Phys. Lett. **90**, 123105 (2007)
5. T.C. Harman, P.J. Taylor, M.P. Walsh, B.E. LaForge: Science **297**, No. 5590, 2229–32 (2002)
6. A.I. Hochbaum, R. Chen, R. Diaz Delgado, W. Liang, E.C. Garnett, M. Najarian, A. Majumdar, P. Yang: Nature **451**, No. 6381, 163–167 (2008)
7. R. Venkatasubramanian, E. Siivola, T. Colpitts and B. O'Quinn: Nature **413**, 597 (2001)
8. C.W. Chang, D. Okawa, A. Majumdar, A. Zettl: Science **314**, No. 5802, 1121–24 (2006)
9. S. Lepri, R. Livi, A. Politi: Physics Reports **377**, 1–80 (2003)
10. M. Toda, R. Kubo: *Statistical Physics II*, Springer Verlag, 2003
11. G.P. Srivastava: *The Physics of Phonons*, Taylor et Francis, 1990

http://www.springer.com/978-3-642-04257-7

Thermal Nanosystems and Nanomaterials
Volz, S. (Ed.)
2009, XX, 588 p. 50 illus., Hardcover
ISBN: 978-3-642-04257-7